Ephemeris Protection Level Equations and Monitor Algorithms for GBAS

Sam Pullen, Jiyun Lee, and Ming Luo

Department of Aeronautics and Astronautics, Stanford University

Boris Pervan, Fang-Cheng Chan, and Livio Gratton

Department of Mechanical, Materials, and Aerospace Engineering, Illinois Institute of Technology

ABSTRACT

One troublesome failure mode for Ground Based Augmentation Systems (GBAS) is the possibility of large discrepancies between satellite locations in space and the locations derived by the ephemeris data that they broadcast. For the Global Positioning System (GPS), nominal ephemeris errors are typically 10 meters or less, and it would take large errors (typically greater than 1 km) to be hazardous to GBAS users making precision approaches to Category I minima. Although most large errors will be detected by the GBAS ground segment Message Field Range Test, ephemeris errors orthogonal to the line-of-sight between a failed satellite and a GBAS ground station are not detectable by this simple test.

To counter this possibility, RTCA has adopted new protection levels to quantify the potential impact of undetected ephemeris failures on user position errors for both precision approach and terminal area applications. These equations define position error bounds as functions of the approximate aircraft location with respect to each satellite and the GBAS ground station as well as the magnitude of the satellite orbit error detectable by the ground station. This Minimum Detectable Error (MDE) determines the "*P*-value" that is broadcast by the GBAS ground station for each satellite it has approved for use.

Several GBAS monitor algorithms have been developed and tested for use in GBAS installations that lack SBAS coverage. One of these is a comparison between satellite positions given by the current satellite ephemeris and the ephemeris broadcast by the same satellite on its previous pass. Variants of this "YE-TE" test have been shown to support GBAS MDE's as low as 1100 meters, which will minimize the resulting impact on Category I user availability due to the ephemeris protection level equations. In addition, means of using raw measurements to initialize this monitor and to separately verify ephemerides in real-time are proposed.

1.0 Introduction: Ephemeris Threat Models

Ground Based Augmentation Systems (GBAS), such as the Local Area Augmentation System (LAAS) being developed by the Federal Aviation Administration, use reference receivers at a single on-airport site to broadcast pseudorange corrections for common-mode errors [1]. Under nominal conditions, GPS satellite ephemeris errors are so small (typically 10 meters or less in 3D, with the along-track direction containing most of the error [2]) that the differential pseudorange error between Ground Based Augmentation System (GBAS) reference receivers and users is negligible. However, this does not preclude the possibility that a failure will cause satellite ephemeris errors large enough to threaten GBAS. If this were to occur, the responsibility for detecting and excluding these failures would lie with the GBAS ground facility rather than with users. To the extent that the ground facility cannot do this, the user must be notified of the magnitude of the possible (undetectable) hazard so that his computed position protection levels include it.

To help validate that GBAS can adequately protect against ephemeris threats, two classes of ephemeris failures have been identified [3]. The failure class designated as "Type A" includes cases where the satellite moves away from its broadcast location due to an un-commanded maneuver, such as a thruster being fired on the satellite without a command being issued by the GPS Operational Control Segment (OCS). While a possible precedent for this type of event exists in the attitude-control thruster "glint firings" that have occurred on SVN's 15 and 18 during eclipse seasons and can cause standalone user range errors as large as 20 meters [4], the resulting errors are too small to concern GBAS. In order to cause errors significant to GBAS, one or more of the more-powerful orbit-maneuvering thrusters would have to fire without being commanded to, and the resulting satellite motion away from its nominal ephemeris would have to go undetected by OCS. Feedback from personnel

inside and outside of OCS indicates that the un-commanded firing of one of the larger thrusters is extremely improbable because it cannot be triggered automatically and because multiple failures would have to occur on the satellite [5].

"Type B" failures, which are considered to be more credible but still very rare, include all cases where no unscheduled maneuver has occurred, but the ephemeris data broadcast is nevertheless incorrect. This event would most likely be caused either by an error in computing the broadcast ephemeris parameters or by corruption of the correct parameters somewhere along the line from OCS creation to OCS satellite uplink to satellite broadcast. Updated GPS navigation data is normally uploaded to each satellite once per day and is composed of 12 "frames" of data that are cycled through at two-hour intervals, with each ephemeris frame being fit to the satellite orbit over a four-hour interval surrounding its broadcast period [6]. Thus, if a Type B fault were to occur, it would become evident at the time of switchover from an old (valid) frame to a new (anomalous) one. When this occurs, GBAS ground stations must validate the new data frame and switch from the old to new frame in its computed pseudorange corrections between 2 and 3 minutes after the new data is received or else exclude the satellite as unhealthy (users see an updated ephemeris CRC to notify them of the switchover and must switch at the same time) [7].

Prior to the introduction of ephemeris protection levels, GBAS ground systems were required to perform a series of sanity checks on navigation when satellites first rise into view and when data switchovers occur, and these monitors are collectively known as "Data Quality Monitoring" (DQM) [8]. These checks confirm that the navigation data itself does not signal a problem and that the new data is consistent with other data (such as the current almanac data or the previous data frame) to within the limits of normal operations. A key contributor to these checks is the Message Field Range Test (MFRT), which simply confirms that the magnitude of the resulting pseudorange corrections is reasonable. Under nominal conditions and with S/A off, these corrections (which are basically the difference between measured pseudorange and computed range based on the broadcast ephemeris) should not exceed a magnitude of about 100 meters. If they do exceed 100 meters, and no other monitor flags have occurred on this satellite, then a large ephemeris error is a strong possibility. This is true for both Type A and Type B failures, as shown in [3]. However, MFRT only observes the component of ephemeris error in the satellite-to-ground-station line of sight; thus it is not guaranteed to detect all threatening ephemeris errors.

This paper develops protection level equations for the ephemeris failure hypothesis that allow GBAS users to compute bounds on possible position errors due to ephemeris failures, provided that the GBAS ground facilities can establish bounds on the magnitude of potentially-undetected ephemeris failures. To establish this bound, a monitor concept has been developed that is now known as the "Yesterday-minus-Today Ephemeris or "YE-TE" test. Several variants of this concept are presented in this paper along with preliminary results from nominal ephemeris data. The YE-TE test is not based on actual measurements and thus cannot detect Type A failures or the "Type AB" hybrid case where erroneous data is broadcast when a satellite is returned to "healthy" status after a deliberate orbit change. These fault cases are considered to be sufficiently improbable that no targeted monitor for these is required to meet the integrity requirements of Category I precision approach [9]. However, this is not likely to remain the case for Category II/III approaches. Measurement-based monitors for this purpose are also presented in this paper, and variants of these monitors can also be used to validate ephemeris messages received after scheduled satellite orbit changes to validate the "YE" in the YE-TE test.

2.0 Derivation of Ephemeris Protection Levels

The effective differential ranging error ($\delta\rho$) due to an error (δe) in knowledge of the line-of-sight unit vector (e) for some satellite i is:

$$\delta\rho_i = \delta e_i^{\mathsf{T}} x \tag{1}$$

where x is the displacement vector between the reference station and user (aircraft) antennas. In turn, the line-of-sight vector error can be expressed directly in terms of satellite position error vector (δr_i) as

$$\delta e_i = \frac{(I - e_i\, e_i^{\mathsf{T}})\, \delta r_i}{r_i}\,, \tag{2}$$

where r_i is the distance (scalar) to satellite i. Substituting equation (2) into (1), we have:

$$\delta\rho_i = \frac{\delta r_i^{\mathsf{T}} (I - e_i\, e_i^{\mathsf{T}})\, x}{r_i} \tag{3}$$

When this error and the other remaining (nominal) error sources (vector v_p below) are projected into the user position domain, the resulting position estimate error for vertical direction will be

$$\delta x_{vert,i} = S_{vert,i} \frac{\delta r_i^{\mathsf{T}} (I - e_i\, e_i^{\mathsf{T}})\, x}{r_i} + S_{vert,:} v_p\,, \tag{4}$$

where $S_{vert,:}$ is the row of the weighted-least-squares projection matrix corresponding to the vertical position state [7]. We consider the vertical case only in this

development; the development for horizontal case is essentially identical.

In writing the first term in equation (4), it is assumed that ephemeris failures occur on only satellite *i*. (We assume that the probability of simultaneous ephemeris failures on more than one satellite is negligibly small). For brevity in notation, we define the 3×3 matrix $E_i \equiv I - e_i\, e_i^{\mathrm{T}}$. It is also noted that $\delta r_i^{\mathrm{T}} E_i\, x$ is a scalar, and that

$$\delta r_i^{\mathrm{T}} E_i\, x \le \| E_i\, x \| \| \delta r_i \| . \tag{5}$$

We assume now that we have available a test statistic (t_e) at the reference station—e.g., almanac-minus-ephemeris position difference—which we may use to infer orbit error magnitude. In this case, a threshold (T_e) on the test statistic may be defined to detect and exclude (at the reference station) a satellite with a large orbit error:

$$T_e = k_{FFA}\sigma_{t_e} . \tag{6}$$

Here, σ_{t_e} is the standard deviation of the nominal test statistic variation (v_{t_e}), and k_{FFA} is a multiplier defined to ensure a specified probability of fault-free alarm (FFA). Defining v_i to be the *i*-th element of v_p, and substituting (5) and (6) into (4), we obtain the following bound on vertical position error:

$$\left|\delta x_{vert,i}\right| \le \left|S_{vert,i}\right| \frac{\| E_i\, x \|}{r_i} k_{FFA}\sigma_{t_e} + \left| S_{vert,i} v_{t_e} + \sum_{j=1}^{n} S_{vert,j} v_j \right| \tag{7}$$

where *n* is the number of satellites used in the position fix. The last term on the right-hand side of (7) is random with standard deviation:

$$\sqrt{S_{vert,i}^2\sigma_{t_e}^2 + \sum_{j=1}^{n} S_{vert,i}^2\sigma_i^2} < S_{vert,i}\sigma_{t_e} + \sqrt{\sum_{j=1}^{n} S_{vert,i}^2\sigma_j^2} , \tag{8}$$

and σ_j is the standard deviation of v_j. Furthermore, it is also true that

$$\| E_i\, x \| \le \| x \| . \tag{9}$$

We next define a missed detection multiplier k_{MD} based on the assumed prior probability of ephemeris error and the tolerable total level of integrity risk. Together with relations (7)-(9) we can now write an upper bound on vertical position error, which we call $VPL_e(i)$ (Vertical Protection Level under the Ephemeris failure hypothesis for satellite *i*):

$$VPL_e(i) \le \left|S_{vert,i}\right| \frac{(k_{FFA}+k_{MD})\sigma_{t_e}}{r_i}\|x\| + k_{MD}\sqrt{\sum_{j=1}^{n} S_{vert,j}^2\sigma_j^2} \tag{10}$$

Within this expression we have the minimum detectable error (*MDE*) in satellite position is

$$MDE = (k_{FFA}+k_{MD})\sigma_{t_e} . \tag{11}.$$

The reference station will broadcast (for each satellite) an ephemeris error decorrelation parameter P_i, [7,14]

$$P_i = MDE/r_i \tag{12}.$$

so that

$$VPL_e(i) \le P_i\left|S_{vert,i}\right|\|x\| + k_{MD}\sqrt{\sum_{j=1}^{n} S_{vert,j}^2\sigma_j^2} . \tag{13}$$

At the aircraft VPL_e is computed as [7]:

$$VPL_e = \max_i VPL_e(i) \tag{14}$$

3.0 VPL_e Impact on GBAS Availability

If ephemeris protection levels are large enough to exceed the nominal-case (H0) protection levels already computed by GBAS users, they will reduce user availability. The degree to which this occurs is a function of the *P*-value, which is derived from the MDE of the ground monitors, and the location of users relative to the ground station. The most critical user location is when the aircraft reaches the end of its approach (the approach threshold), where the tightest VAL (10 m for Category I) applies [9]. Note that the displacement $x_{RR\text{-}GPIP}$ between the centroid of the reference receivers and the glide path intercept point (GPIP) is needed to define *x* in (13).

A study of the impact of VPL_e on GBAS Category I availability was reported in [12]. For $x_{RR\text{-}GPIP}$ = 3 n.mi. (about 5.5 km), which should suffice for most airports, there is no availability impact (VPL_e is smaller than VPL_{H0}) for *MDE* ≤ 1900 m. Above this value, a slight loss of availability appears but does not become significant until the *MDE* reaches 4000 meters or so. This conclusion was based on k_{MD} = 3.7. Further analysis in [13] has shown that k_{MD} = 3.1 (to provide a missed-detection probability of 0.001) is acceptable; thus the actual *MDE* that will cause availability loss are somewhat higher. These results provide guidance regarding the

ephemeris MDE that will be acceptable in operation, and the methods developed in the following sections are intended to reduce the ephemeris *MDE* such that little if any GBAS availability is lost.

4.0 YE-TE Derivation and Evaluation Results

4.1 YE-TE Concept and Capabilities

The concept of the YE-TE test is simply to confirm that today's broadcast ephemeris data for each GPS satellite is correct by comparison with the most recent ephemeris data that has already been validated. For a satellite that is already in view and has an ephemeris frame change, the comparison is between the new and immediately previous sets of data, and under nominal conditions, these agree to within several meters during the 2-hour period within the "fit intervals" of both sets of data [3]. However, when a satellite first rises in view of the GBAS ground station, the most recent validated data is from the previous pass of that satellite and may be as much as 24 hours old. Thus, it is long past its "fit interval" and no longer precisely indicates the satellite location. Nevertheless, it is a valid basis for comparison within the limits of its accuracy. If the new ephemeris is dramatically in error, as in the "Type B" failure defined in Section 1.0, this comparison will detect the failure.

YE-TE comparisons can be based on satellite positions computed from the old and new ephemerides or the individual orbit parameters of the old and new messages. The former approach is detailed in Sections 4.2 and 4.3, while the latter approach is introduced in Section 4.4. Note that the focus of both methods is on validating ephemerides for newly risen satellites. The impact of incorrectly rejecting a satellite with a healthy ephemeris is that the use of a healthy satellite is lost, but continuity is not affected because rejection would occur before the satellite is approved for use that day. Therefore, the YE-TE fault-free alarm probability need not be low enough to fit within the LGF continuity allocation. Instead, it should be small compared to the probability that a given satellite will be flagged unhealthy (and thus unusable) when it rises into view. Based on an analysis in [16], P_{FFA} can be set to 1.9×10^{-4} per newly risen satellite, which gives k_{FFA} = 3.73 provided that a Gaussian extrapolation can be used. During ephemeris changeovers for already-approved satellites, continuity is at risk if the satellite is rejected; thus P_{FFA} must fit within the overall continuity requirement of 8×10^{-6} per 15 seconds [14]. The nominal ephemeris differences are much lower in this case; thus this lower P_{FFA} does not require an increase in *MDE*.

4.2 Baseline YE-TE Algorithm and Results

First, define $x_{TE}(t_1)$ as a vector containing the three components of the position of a given satellite in the intrack-crosstrack-radial or "local level" (LL) orbit-referenced frame at time t_1, based on the latest (to-be-validated) ephemeris, and define $x_{YE}(t_1)$ similarly but based on the previous, already-validated ephemeris. These satellite positions are first computed in the Earth-Centered Earth-Fixed (ECEF) reference frame using the standard algorithm defined in Section 20.3.3.4.3 of GPS ICD-200C [15] and are then rotated into the LL frame [17]. A "single-difference" vector of YE-TE position differences in each axis can be created for a vector of times t that covers the visibility period of interest:

$$SD(t) = x_{TE}(t) - x_{YE}(t) \qquad (15)$$

The maximum of *YETE* in each axis over the time period covered by t is the test statistic for that axis. Thresholds can be set individually for each axis (denote this as "X_{SD}"), or the RSS of the values for each axis (denote this as "Z_{SD}") can be used to compare to a single threshold. The latter is more convenient, as it directly translates into the scalar *MDE* value used to compute VPL_e.

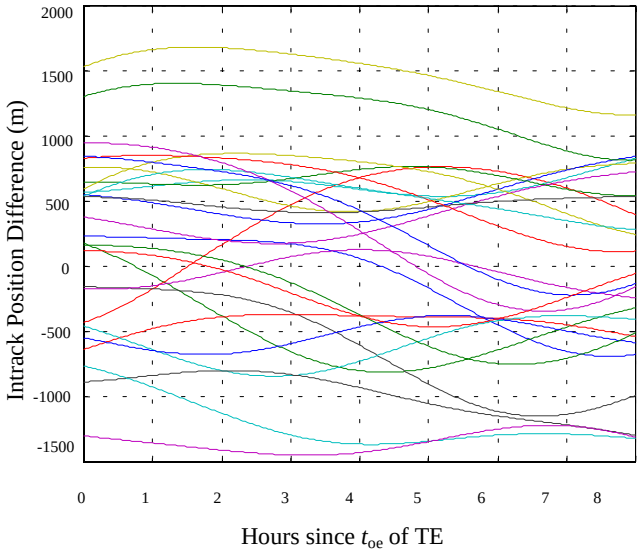

Figure 1: Example YE-TE Results for Intrack Axis

Figures 1, 2, and 3 show plots of the intrack, crosstrack, and radial components of *SD*, respectively, where satellite positions computed from ephemerides received at the Colorado Springs IGS site "amc2" on January 10, 2001 are compared to ephemerides with a time-of-ephemeris (t_{oe}) 24 hours earlier. In each case, the vector t runs from

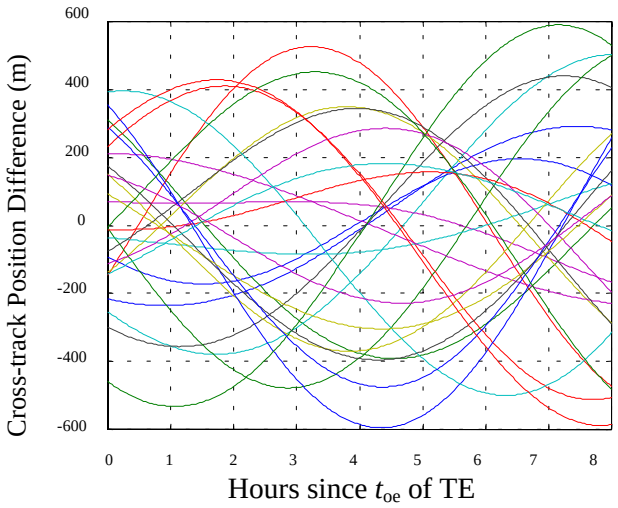

Figure 2: Example YE-TE Results for Crosstrack Axis

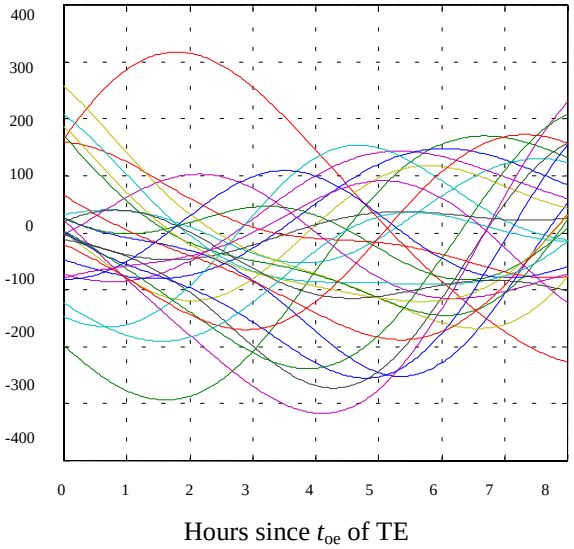

Figure 3: Example YE-TE Results for Radial Axis

the t_{oe} of the new ephemeris to a time 8 hours later (long enough to cover any satellite pass) at 5-minute intervals. Under nominal conditions, the position differences shown in these plots are due to orbit perturbations that take place during the period from t_{oe} of YE to t_{oe} of TE, since it is known that nominal ephemeris messages are very accurate within their fit intervals [2]. The intrack differences are the largest and therefore dominate the combined test statistic Z_{SD}. While the crosstrack and radial differences are dominated by "short-period" oscillations with periods of less than a day, the intrack differences show both short and long-period oscillations (the long-period oscillations dictate the non-zero mean of the intrack differences). These effects are discussed in more detail in Section 4.4.

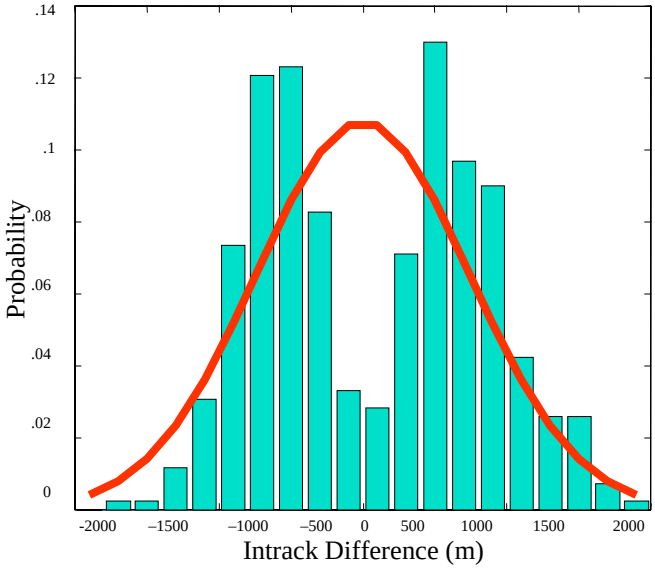

Figure 4: YE-TE Histogram for Intrack Axis

Figure 4 shows a histogram of X_{SD} in the intrack axis for all valid satellite ephemerides received at Colorado Springs from January 7 through February 17, 2001 (a total of 423 separate YE-TE test results). Satellites undergoing maintenance (and possible orbit changes) were excluded from these results based on NANU's issued by OCS. Note that the test statistic distributions are bimodal – typical values are on either side of zero rather than centering about zero. However, the Gaussian distribution with zero mean and the sample standard deviation (746.2 m in Figure 4; the crosstrack and radial values are 398.9 m and 165.6 m, respectively) shown in red appears to overbound the observed bimodal distributions in the tails. Thus, thresholds and MDE's derived from the Gaussian extrapolations in (11) should be sufficient, pending validation with more data points.

Because these YE-TE differences are driven by orbit perturbations with periodic behavior, they can be reduced somewhat by exploiting this expected periodicity. A "double-difference" YE-TE can be formed as follows:

$$DD(t) = SD(t_{TE}) - SD(t_{YE}) \qquad (16)$$

This new statistic differences out the *SD* vector computed for the 8 hours since the t_{oe} of YE from the standard definition of *SD* in (15), which is computed for the 8 hours since the t_{oe} of TE. This has the effect of differencing out short-term oscillations, and the result for the intrack axis is shown in Figure 5. The short-term oscillations visible in Figure 1 are now almost completely absent – what remains is the orbit change due to the long-

term oscillations, and these differences are reduced as well. Over a longer dataset from January 7 to May 15, 2001 (1312 YE-TE test results), the X_{DD} intrack standard deviation is 527.9 meters (27% lower than that for X_{SD}). Although oscillations do not disappear from the crosstrack and radial *DD* results because multiple asynchronous short-term oscillations exist, the standard deviations in these axes are reduced to 315.2 and 6.3 meters, respectively (the radial reduction is surprisingly large).

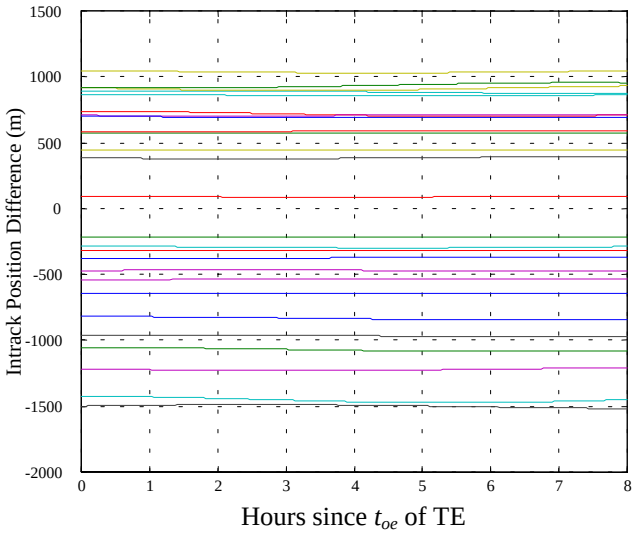

Figure 5: Double-Difference YE-TE Results for Intrack Axis

Finally, if the ephemeris for a newly risen satellite was validated by the YE-TE test when it rose on the previous day, the YE-TE test result from the previous day can be used to create a "triple difference" as follows:

$$TD(t) = DD(t_{TE}) - DD(t_{YE}) \qquad (17)$$

where, in this context, $DD(t_{TE})$ represents the double-difference YE-TE result vector for today's pass of the satellite in question, and $DD(t_{YE})$ represents the same result for yesterday's pass (i.e., it is the YE-TE result from yesterday's validation of the satellite). When $DD(t_{YE})$ exists, *TD* linearly extrapolates the orbit change apparent in yesterday's result forward another day and subtracts out this "predicted" change. During the "trending" part of the long-term oscillation, X_{TD} will generally be lower than X_{DD} along the intrack axis, but this will not be true near the peaks of this oscillation, when X_{DD} will generally be smaller. Therefore, it makes sense to use the smaller of X_{TD} and X_{DD} (denote this as X_{Dmin}) when it is possible to compute *TD*. Because the crosstrack and intrack axes do not share the long-term periodicity of the intrack axis, computing *TD* has relatively little impact on these axes.

When X_{TD} is smaller than X_{DD}, its standard deviation in the intrack direction is reduced to only 264.3 meters, which is now lower than that of the crosstrack direction (the radial direction is still negligible). Over all cases where X_{TD} can be computed (whether or not it is smaller), the intrack and crosstrack standard deviations are 336.6 meters and 312.3 meters, respectively; thus both contribute to the scalar value Z_{Dmin}.

4.3 Orbit-Fitting YE-TE Algorithm and Results

The YE-TE methods defined in Section 4.2 attempt to indirectly remove predictable satellite orbit changes using double and triple-differences. In theory, a preferable method is to directly model the expected perturbations using orbit theory. While orbit determination from a single observation site is not accurate enough to use as a GBAS ephemeris monitor, orbit fitting applied to the satellite locations computed from the original YE during its 4-hour fit interval is highly accurate because the input "measurements" were accurate to within a few meters in 3-D (as opposed to in the line-of-sight direction only using pseudorange measurements) if YE was valid yesterday. Dynamic orbit-perturbation models are then used to fill in the gap between the time of applicability of YE and today's t_{oe} so that an "improved" version of YE (denote it as YE') is available to compare to TE.

This method has been evaluated using Microcosm® software for orbit fitting and propagation. A 3×2 expansion of the standard JGM-3 Earth gravity model combined with the Microcosm® solar radiation pressure model is sufficient to achieve the needed orbit-determination accuracy (including Sun and Moon gravity perturbations as well does not significantly improve the resulting YE-TE values). Applying this technique to create YE' and then substituting YE' for YE in (15) (note that *DD* and *TD* are not needed) reduces the cross-track and radial YE-TE values to about 10 meters (1σ) and makes them negligible compared to the intrack YE-TE value, which has an RMS value of 166.3 meters. Example intrack results for 29 YE-TE pairs between January 9 and January 12, 2001 are shown in Figure 6. As in the *DD* results of Figure 5, this orbit-fitting technique removes most of the long-period oscillation. A mean offset of about –85 meters is visible in Figure 6 and consistently appears in data from other days in January. Subtracting this offset from the test statistic leaves a standard deviation of 145.3 meters. Since the other two axes are negligible, and the results are no longer strongly bimodal, a Gaussian extrapolation with $k_{FFA} = 3.73$ and $k_{MD} = 3.1$ can be used with (11) to derive an MDE of about 1000 – 1100 meters for this test.

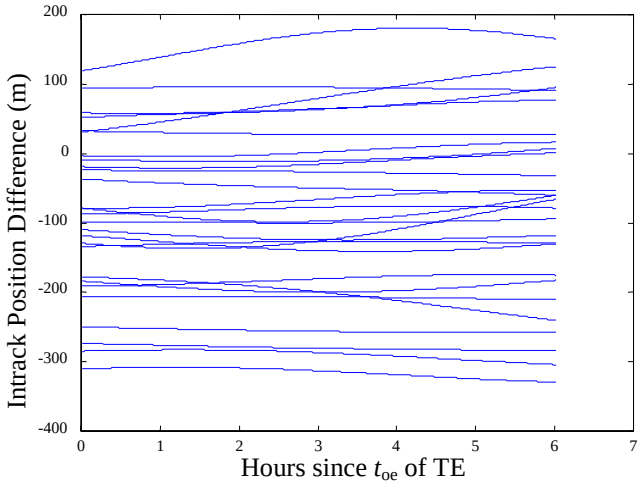

Figure 6: Orbit-Fitting YE-TE Results for Intrack Axis

Figure 7 summarizes the achievable ephemeris MDE's demonstrated thus far for the YE-TE test variants discussed above as well as their qualitative impact on user availability. An MDE of 3000 – 4000 meters can be achieved by the *DD* and *TD* YE-TE variations described in Section 4.2. This implies only a small loss of Category I user availability. The orbit-fitting method of Section 4.3 produces MDE's small enough to cause no loss of Category I availability for almost all GBAS-equipped airports. Its primary disadvantage is software complexity. Implementing orbit fitting in a GBAS ground facility would significantly complicate the software and add to its processing load. Therefore, it may be preferable to use the simpler YE-TE methods of Section 4.2 in Category I GBAS systems.

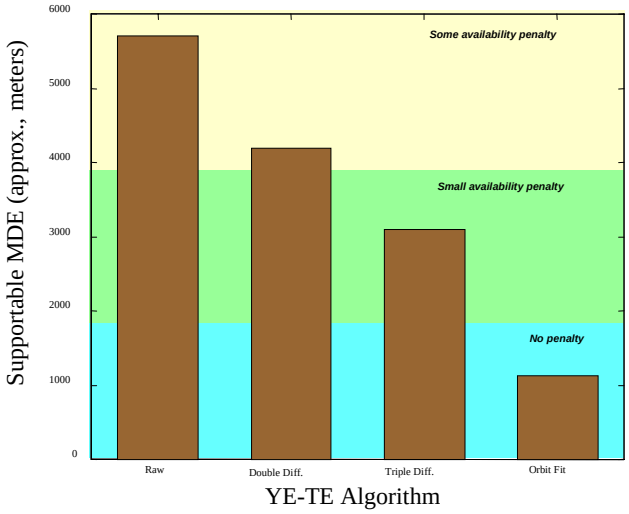

Figure 7: YE-TE Based Ephemeris MDE Values

4.4 Parameter-Based YE-TE Methods

The YE-TE implementations considered thus far have involved tests in the satellite position domain. In this section, we introduce some preliminary concepts of an alternative approach based on the direct comparison of current broadcast ephemeris *parameters* with those previously broadcast and validated. The advantage of a parameter-based approach is that it is easier to observe and quantify variations in orbit parameters than satellite position, because the latter changes continuously in time for a fixed parameter set. Parameter-based approaches may eventually provide improved performance over basic position-based YE-TE algorithms (Sections 4.1 and 4.2), while offering a lower level of complexity than position domain orbit fitting approaches (Section 4.3). Furthermore, the performance of parameter-based tests can also be easily expressed in position domain (needed to define the MDE and *P*-value) as described below.

Given the time-of-ephemeris (t_{oe}) and the fifteen broadcast ephemeris parameters

$$[p_1, \ \ldots \ , p_{15}] = [A, \ M_0, \Delta n, e, \Omega_0, I_0, IDOT, \ldots] \quad (18)$$

we can compute the satellite position (x, y, z) at any time t:

$$\begin{bmatrix} x(t) \\ y(t) \\ z(t) \end{bmatrix} = \begin{bmatrix} f(p_1, \ldots, p_{15}, t_{oe}, t) \\ g(p_1, \ldots, p_{15}, t_{oe}, t) \\ h(p_1, \ldots, p_{15}, t_{oe}, t) \end{bmatrix} = \begin{bmatrix} f(p, t_{oe}, t) \\ g(p, t_{oe}, t) \\ h(p, t_{oe}, t) \end{bmatrix} \quad (19)$$

where p is the parameter vector (15 elements), and the nonlinear functions f, g, and h in equation (19) are defined by the satellite position algorithms in GPS ICD-200C [15].

Now consider sensitivity to parameter variations:

$$\begin{bmatrix} \delta x(t) \\ \delta y(t) \\ \delta z(t) \end{bmatrix} = \begin{bmatrix} \frac{\partial f(p,t_{oe},t)}{\partial p_1} & \cdots\cdots & \frac{\partial f(p,t_{oe},t)}{\partial p_{15}} \\ \frac{\partial g(p,t_{oe},t)}{\partial p_1} & \cdots\cdots & \frac{\partial g(p,t_{oe},t)}{\partial p_{15}} \\ \frac{\partial h(p,t_{oe},t)}{\partial p_1} & \cdots\cdots & \frac{\partial h(p,t_{oe},t)}{\partial p_{15}} \end{bmatrix} \begin{bmatrix} \delta p_1 \\ \vdots \\ \delta p_{15} \end{bmatrix} . \quad (20)$$

In a more compact form, we can write

$$\delta r(t) = Q(p, t_{oe}, t)\, \delta p \quad (21)$$

where Q is the 3×15 sensitivity matrix in equation (20), which may be computed by either numerical or analytical partial differentiation of f, g, and h. Equation (21) is a linearized expression directly relating parameter and position variation.

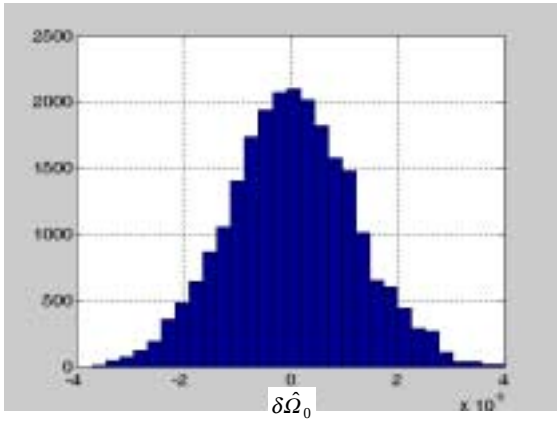

(a) Nearly Gaussian: $\sigma = 1.2 \times 10^{-5}$

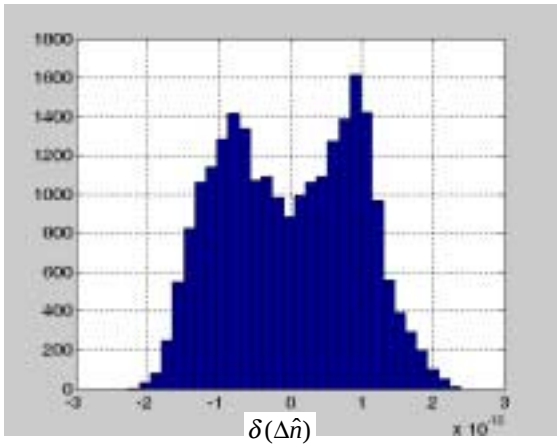

(b) Bi-Modal: $\sigma = 9.3 \times 10^{-11}$ s^{-1}

Figures 8: Example Distributions of Parameter Variation

Defining the broadcast parameter vector as p_b and the true parameter vector as p, the parameter variation vector is $\delta p = p_b - p$. While we cannot measure p directly, we can use prior parameter sets to obtain an estimate $\hat{p}$, such that $\delta\hat{p} = p_b - \hat{p}$. Ideally, we desire that under normal conditions (no ephemeris failure) that $\delta\hat{p}$ is small in a statistical sense (i.e., that our *estimate* of p is a good one). In this case, we may set tight fault-detection thresholds without incurring high false alarm rates.

We first consider the simplest possible estimator of orbit parameter error on day k, by following the basic YE-TE approach of using the prior day's ephemeris parameter set (i.e., from 24 hours earlier) as the estimate of the current parameter set. In this case:

$$\hat{p}(k) = p_b(k-1) \quad \Rightarrow \quad \delta\hat{p}(k) = p_b(k) - p_b(k-1) \quad (22)$$

Using archived broadcast ephemeris data we can obtain empirical distributions for $\delta\hat{p}$. Example histograms for two parameters (Ω_0 and Δn) are shown in Figures 8 (a) and (b). The distributions shown are typical of the remaining parameters in the sense that some distributions exhibit nearly Gaussian behavior while others show bi-modal characteristics seen in the $\delta(\Delta n)$ histogram. The bimodal structure of the latter distribution suggests that an underlying sinusoidal variation in the parameter may exist. This observation is verified by directly plotting broadcast Δn against time (in days). Figure 9 shows the time history of this parameter sampled at 24-hour intervals. The strong harmonic structure (with approximately a 14-day period) clearly suggests that the use of the prior day's value of the parameter Δn is generally a rather poor estimator the current day's value of the parameter. For this parameter, it is obvious that a sinusoid projection model will produce better results.

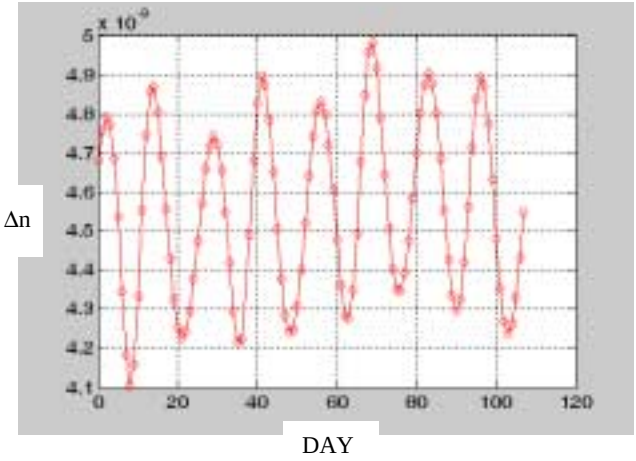

Figure 9: Broadcast Δn vs. t_{oe} (24-hour sample period)

It is important to note however, that more precise projection models will come at the expense of some increase in implementation complexity (although undoubtedly less than orbit-fitting approaches). In return, however, the prospect of tighter and better-behaved distributions of parameter estimate error may ultimately yield lower MDEs and *P*-values than basic (non-orbit-fitting) YE-TE approaches. These tradeoffs are currently being investigated, and the results will be documented in a future paper.

5.0 Measurement-Based Initialization Monitor

Regardless of the particular YE-TE implementation used, it is true that after a scheduled station-keeping maneuver, no valid prior ephemeris will be available to test current broadcast ephemeris. In this event, one potential solution is to validate the post-maneuver broadcast ephemeris using existing LAAS Ground Facility (LGF) code and carrier measurements. To determine whether or not such an approach is effective,

we will assume that we have one day available immediately following the maneuver (during which corrections will not be broadcast) to validate the current ephemeris. If validated, this ephemeris may be used on the following day in a YE-TE-type monitor implementation.

The reference receiver measurements we consider here are:

(a) *Standalone Pseudorange Residual* (i.e., the broadcast pseudorange correction), which measures the orbit error over time (k) projected into the satellite's line-of-sight direction:

$$z_k^\rho = e_k^\mathsf{T}\,\delta r_k + \upsilon_k^\rho \tag{23}$$

(b) *Differential Carrier Residuals* (across existing reference receiver baselines), which measure orbit error over time orthogonal to the line-of-sight, projected into the baseline directions. We assume two orthogonal baselines of length ℓ with unit vector directions defined by the columns of matrix B in the double difference equation below:

$$z_k^\phi = \ell\,\frac{B^\mathsf{T} E_k}{r_k}\,\delta r_k + \lambda N + \upsilon_k^\phi \tag{24}$$

For simplicity in notation we define $A_k \equiv B^\mathsf{T}E_k/r_k$. Given a single-frequency LGF (the nominal case), we assume integers are unknown, so we form a triple difference observable instead:

$$y_k^\phi \;=\; z_k^\phi - z_0^\phi \;=\; \ell\;A_k\,\delta r_k - \ell\;A_0\,\delta r_0 + \overline{\upsilon}_k^\phi \tag{25}$$

Consider now an initial (small) deviation in satellite position and velocity from a circular Keplerian orbit—a first approximation of the GPS orbit. In this case, future positions are defined by the well-known Euler-Hill transition matrix G_k [19]:

$$\delta r_k = G_k \begin{bmatrix} \delta r_0 \\ \delta v_0 \end{bmatrix} = G_k \delta s_0 \tag{26}$$

Our measurements (23) and (25) may now be expressed as:

$$z_k^\rho \;=\; e_k^\mathsf{T}\;G_k\,\delta s_0 + \upsilon_k^\rho \;\equiv\; C_k \delta s_0 + \upsilon_k^\rho \tag{27}$$

$$y_k^\phi \;=\; \ell\,(A_k G_{\,k} - A_0 G_0)\,\delta s_0 + \overline{\upsilon}_k^\phi \;\equiv\; \ell\,D_k \delta s_0 + \overline{\upsilon}_k^\phi \tag{28}$$

We now may stack measurements for one day to estimate δs_0 and obtain the associated estimate error covariance matrix cov(δs_0). The covariance on SV position error at time k is then:

$$\mathrm{cov}(\delta r_k) \;=\; G_k\,\mathrm{cov}(\delta s_0)\,G_k^\mathsf{T}\,, \tag{29}$$

and the minimum detectable ephemeris error for time k is:

$$MDE_k = (k_{FFA} + k_{MD})\left\|\mathrm{cov}(\delta r_k)\right\|_2^{1/2} \tag{30}$$

Figure 10 shows covariance simulation results using the full DO-229A GPS constellation [18] for a Chicago O'Hare LGF installation assuming:

- Independent samples collected at 5 min intervals;
- 5 deg elevation mask
- σ_ρ = 30 m (pseudorange correction with S/A)
- σ_ϕ = 0.01 m (differential carrier/integer unknown)
- k_{FFA} = 3.73 and k_{MD} = 3.1 (the same values used for previous YE-TE results)

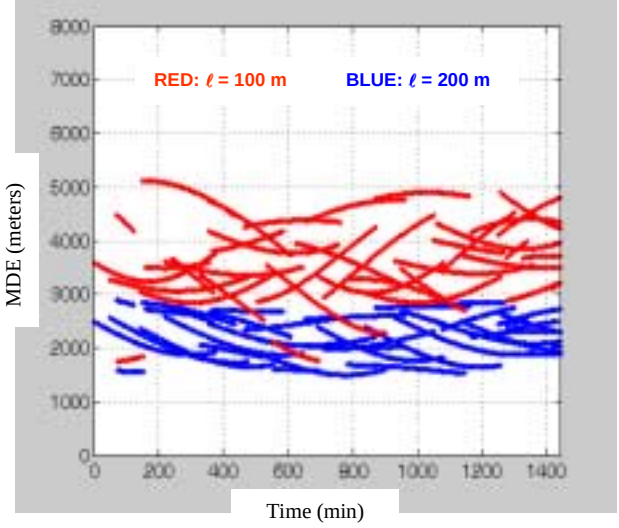

Figure 10: MDE Results for Initialization

The results shown in Figure 10 are particularly encouraging because MDE values are within the same range as those expected for basic YE-TE monitors. Although Keplerian orbits have been assumed so far, the GPS satellite orbit model can be used instead by replacing:

- Euler-Hill transition matrix (G) with the parameter sensitivity matrix (Q).
- Initial state vector error (δs_0) with orbit parameter error vector (δp).

It should also be noted that if the carrier cycle ambiguity for the (post-maneuver) rising satellite can be resolved, long initialization times (e.g., one day assumed in our analysis above) are not necessary. The use of multipath limiting antennas (MLAs) in the LGF may be

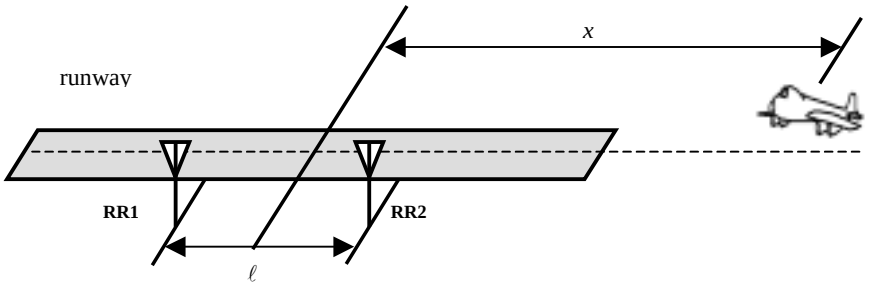

Figure 11: Baseline-Runway Configuration

particularly beneficial in this regard. Furthermore, as discussed in the next section, with a dual-frequency LGF, a similar technique can be used to provide the means for real-time monitoring for both Type A and Type B ephemeris events.

6.0 Measurement-Based Real-Time Monitor

Consider a single reference receiver baseline aligned with a runway as shown in Figure 11. This simple configuration is assumed for clarity in the development which follows. (When two orthogonal baselines are used, the specific runway orientation is irrelevant.) Given an orbit error on a satellite, δr_k (at time k), the effective pseudorange (PR) error seen by the aircraft is:

$$\delta PR_k = x(A_k\, \delta r_k) + \upsilon_k^{PR} \qquad (31)$$

Of course, the orbit error is also observable in the double difference carrier at the LGF:

$$z_k^{\phi} = \ell(A_k\, \delta r_k) + \lambda N + \upsilon_k^{\phi} \qquad (32)$$

Assuming the cycle ambiguity is *known*, we can set a threshold on double-difference carrier residual to observe and detect orbit error in real-time. The resulting minimum detectable value of $A_k \delta r_k$ is just the broadcast P-value, and may be expressed as follows:

$$P = (k_{FFA} + k_{MD})\frac{\sigma_{\phi}}{\ell} \qquad (33)$$

This result can also be expressed as an MDE using equation (12). Note that this is a real-time monitor, so k_{FFA} is driven by continuity (not availability) considerations. For the purposes of this analysis, we assume that for this monitor $P_{\text{FFA}} \approx 10^{-9}$ (k_{FFA} = 6.1). Figure 12 shows the resulting MDE as a function of reference receiver baseline length for two example carrier measurement error cases. Good performance (as measured by YE-TE performance results) is achievable for baselines of 200 – 400 m. Furthermore, it should again be noted that this performance applies for both Type A and B ephemeris failures, in contrast with the YE-TE approaches that are effective against Type B failures only.

To ensure adequate satellite availability, the cycle ambiguity for a rising SV must be resolved quickly, because the LGF cannot approve the SV for use until the first carrier residual test is passed. Furthermore, a *geometry-free* cycle resolution method is required, because it cannot be assumed that broadcast ephemeris is correct. With a single-frequency LGF (the current Category I standard), code-minus-carrier measurements may be averaged to estimate the cycle ambiguity, but the averaging times needed are excessively long for the real-time implementation under consideration. (However, as noted in the last section, such an approach may be acceptable for YE-TE initialization.)

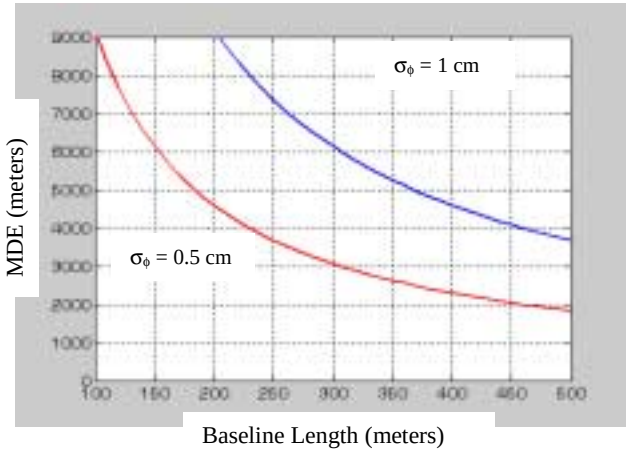

Figure 12: MDE Results for Real-Time Monitoring

With a *dual-frequency* LGF (still an option for Cat II/III), the L1 cycle ambiguity for a rising satellite can be resolved much more quickly by resolving the L1-L2 widelane integer as an intermediate step. The required probability of correct resolution is set by availability requirements (~ 0.999). If the integer is incorrectly

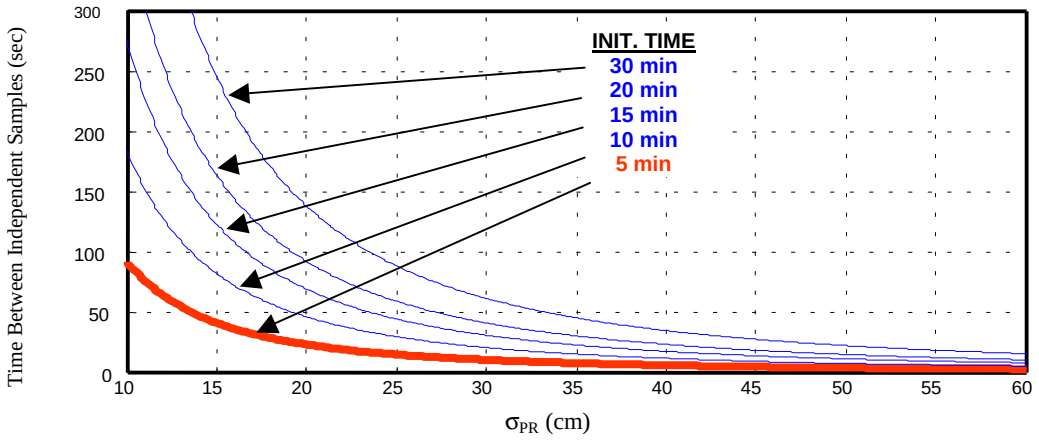

Figure 13: Required PR Error for Real-Time Implementation

resolved, the ephemeris test will alarm before a satellite is approved. To ensure the required correct resolution probability, some averaging will still be required. The initialization time is primarily driven by successful widelane integer resolution, which in turn, will depend principally on the pseudorange measurement error standard deviation and correlation time (or, alternatively, the interval between independent samples).

Figure 13 shows the minimum requirements on pseudorange measurement error and independent sample interval to achieve a specified initialization time. It is obvious that as the desired initialization time is lowered, the requirements on measurement error become more stringent. It is anticipated that the error performance of dual-frequency MLA antennas currently under development will be good enough to support initialization within approximately 5 minutes.

7.0 Conclusions and Future Work

This paper has defined Type A (undesired maneuver) and Type B (erroneous data) threat models for satellite ephemeris errors large enough to threaten GBAS users and has derived ephemeris protection levels that connect the magnitude of potential ephemeris errors to the impact on user position. These protection levels will be required in future GBAS standards. GBAS ground system ephemeris monitoring supports a "Minimum Detectable Error" (MDE) bound on the size of Type B errors that may not be detected with the required missed-detection probability (Type A errors are considered to be extremely improbable). More-effective monitoring translates into lower MDE's and P-values, which leads to lower ephemeris protection levels and a lesser impact on GBAS user availability.

To detect Type B ephemeris failures, satellite-position-based and orbit-parameter-based YE-TE tests have been introduced. The simpler position-based methods are sufficient to limit, but not eliminate, Category I availability loss due to the addition of VPL_e. The orbit-fitting YE-TE variant reduces the ephemeris MDE enough to practically eliminate this availability loss, but this method would be complex and expensive to implement in a real-time GBAS ground station. To evaluate the practicality of this approach, orbit-fitting algorithms are being implemented in the Data-Quality-Monitoring (DQM) segment of Stanford's GBAS ground system prototype, the Integrity Monitor Testbed (IMT) [3,8]. Parameter-based methods have also been developed and show promise, using simple propagation models, to achieve lower MDEs than the basic (non-orbit-fitting) position-based approaches. Parameter-based methods will continue to be investigated to determine if an attractive tradeoff exists between MDE performance and projection- model complexity.

Measurement-based approaches to initialize the YE-TE monitor after scheduled SV maneuvers have been investigated. The resulting MDE estimates are consistent with predicted YE-TE test performance, suggesting that the LGF measurements may provide a practical means of validating a single ephemeris message so that it can be used as "YE" to approve subsequent ephemeris updates. The relevant algorithms are currently being refined to accommodate non-Keplerian orbit effects.

A real-time measurement-based approach toward ephemeris failure detection has also been defined and may be suitable for Category II/III GBAS implementation. The method uses differential carrier phase measurements across LGF reference receiver baselines and is capable of detecting both Type A and Type B failures. However, dual-frequency reference receivers are required to resolve integers within a time frame that is practical for a real-time monitor, and the baselines between reference receiver antennas will likely need to be longer than currently envisioned. Demonstration and validation of this technique will continue to better quantify its effectiveness and its impact on GBAS design.

ACKNOWLEDGMENTS

The authors would like to thank Todd Walter and Gang Xie for their help during this research. This work was also supported by the efforts of Barbara Clark of FAA AIR-130, Tom Hsiao, Curt Shively, Chris Varner, and Ron Braff of MITRE, Victor Wullschleger and John Warburton of FAA ACT-360, and others participating in RTCA SC-159 WG-4 requirements development. The advice and interest of many other people in the Stanford GPS research group is appreciated, as is funding support from the FAA LAAS Program Office (AND-710). The opinions discussed here are those of the authors and do not necessarily represent those of the FAA or other affiliated agencies.

REFERENCES

[1] R. Braff, "Description of the FAA's Local Area Augmentation System (LAAS)," *Navigation*. Vol. 44, No. 4, Winter 1997-98, pp. 411-424.

[2] D. Jefferson, Y. Bar-Sever, "Accuracy and Consistency of Broadcast GPS Ephemeris Data," *Proceedings of ION GPS 2000*. Salt Lake City, UT., Sept. 19-22, 2000, pp. 391-395.

[3] S. Matsumoto, S. Pullen, M. Rotkowitz, B. Pervan, "GPS Ephemeris Verification for Local Area Augmentation System (LAAS) Ground Stations," *Proceedings of ION GPS-99*. Nashville, TN., Sept. 14-17, 1999, pp. 691-704.

[4] M. Rivers, "2 SOPS Anomaly Resolution on an Aging Constellation," *Proceedings of ION GPS 2000*. Salt Lake City, UT., Sept. 19-22, 2000, pp. 2547-2550.

[5] S. Pullen, et.al., "Minutes of 2SOPS/FAA Interoperability Meeting." Colorado Springs, CO.: ARINC, Unpublished Manuscript, Version 3.0, Feb. 3, 1999.

[6] J. Spilker, "GPS Navigation Data," in B. Parkinson and J. Spilker, Eds., *Global Positioning System: Theory and Applications*. Washington, D.C.: AIAA, 1996. Volume I, Chapter 4, pp. 121-176.

[7] *Minimum Operational Performance Standards for GPS Local Area Augmentation System Airborne Equipment*. Washington, D.C.: RTCA SC-159 WG-4A, DO-253, January 11, 2000.

[8] G. Xie, *et.al.*, "Integrity Design and Updated Test Results for the Stanford LAAS Integrity Monitor Testbed," *Proceedings of the ION 57th Annual Meeting*. Albuquerque, NM., June 11-13, 2001, pp. 681-693.

[9] *Minimum Aviation System Performance Standards for the Local Area Augmentation System*. Washington, D.C.: RTCA SC-159, WG-4A, DO-245, Sept. 28, 1998.

[10] B. Parkinson, "GPS Error Analysis," in B. Parkinson and J. Spilker, Eds., *Global Positioning System: Theory and Applications*. Washington, D.C.: AIAA, 1996. Volume I, Chapter 11, pp. 469-483.

[11] S. Pullen, M. Rotkowitz, "OCS Monitoring Effectiveness and LAAS Ephemeris Requirements," Department of Aeronautics and Astronautics, Stanford University, Version 1.1, March 4, 1999.

[12] T. Hsiao, C. Shively, C. Varner, "LAAS Ephemeris Error Protection Requirements & Availability (Draft Revision 1)." MITRE/CAASD, February 26, 2001.

[13] C. Shively, "Integrity from Ephemeris Test and Protection Level," MITRE/CAASD, Draft Manuscript, March 8, 2001.

[14] *Specification: Category One Local Area Augmentation System Non-Federal Ground Facility*. Washington, D.C.: U.S. Dept. of Transportation, Federal Aviation Administration, FAA/AND710-2937, May 31, 2001.

[15] *NAVSTAR GPS Space Segment / Navigation User Interfaces*. El Segundo, CA., ARINC Research Corp., GPS-ICD-200C, October 10, 1993. Available at: http://www.navcen.uscg.gov/pubs/gps/icd200/icd200cw1234.pdf

[16] S. Pullen, "False-Rejection Probability Requirements for Initial GPS Satellite Acquisition," Stanford University, Draft Version 1.1, May 17, 2001.

[17] D. Vallado, *Fundamentals of Astrodynamics and Applications*. New York: McGraw Hill, 1997. Section 1.4, pp. 31-44.

[18] *Minimum Operational Performance Standards for Global Positioning System/Wide Area Augmentation System Airborne Equipment*. Washington, D.C.: RTCA SC-159 WG-2, DO-229B, October 6, 1999, Appendix B.

[19] M. Kaplan, *Modern Spacecraft Dynamics and Control*. New York: John Wiley and Sons, 1976. Section 3.6, pp. 108-115.